

# In vivo quantitative analysis of Talin turnover in response to force

Guðlaug Katrín Hákonardóttir<sup>a,\*</sup>, Pablo López-Ceballos<sup>a,\*</sup>, Alejandra Donají Herrera-Reyes<sup>b</sup>, Raibatak Das<sup>c</sup>, Daniel Coombs<sup>b</sup>, and Guy Tanentzapf<sup>a</sup>

<sup>a</sup>Department of Cellular and Physiological Sciences, Life Science Institute, University of British Columbia, Vancouver, BC V6T 1Z3, Canada; <sup>b</sup>Department of Mathematics and Institute of Applied Mathematics, University of British Columbia, Vancouver, BC V6T 1Z2, Canada; <sup>c</sup>Department of Integrative Biology, University of Colorado Denver, Denver, CO 80204

**ABSTRACT** Cell adhesion to the extracellular matrix (ECM) allows cells to form and maintain three-dimensional tissue architecture. Cell–ECM adhesions are stabilized upon exposure to mechanical force. In this study, we used quantitative imaging and mathematical modeling to gain mechanistic insight into how integrin-based adhesions respond to increased and decreased mechanical forces. A critical means of regulating integrin-based adhesion is provided by modulating the turnover of integrin and its adhesion complex (integrin adhesion complex [IAC]). The turnover of the IAC component Talin, a known mechanosensor, was analyzed using fluorescence recovery after photobleaching. Experiments were carried out in live, intact flies in genetic backgrounds that increased or decreased the force applied on sites of adhesion. This analysis showed that when force is elevated, the rate of assembly of new adhesions increases such that cell–ECM adhesion is stabilized. Moreover, under conditions of decreased force, the overall rate of turnover, but not the proportion of adhesion complex components undergoing turnover, increases. Using point mutations, we identify the key functional domains of Talin that mediate its response to force. Finally, by fitting a mathematical model to the data, we uncover the mechanisms that mediate the stabilization of ECM-based adhesion during development.

## Monitoring Editor

Valerie Marie Weaver  
University of California,  
San Francisco

Received: May 21, 2015

Revised: Oct 1, 2015

Accepted: Oct 1, 2015

## INTRODUCTION

A fundamental question in biology is how tissues maintain their structure in the face of the constant strain, tension, and deforming mechanical forces imposed by the external environment. Integrin-mediated adhesion is essential for maintaining tissue integrity by anchoring cells to the extracellular matrix (ECM) when tissues are

exposed to mechanical force (Papusheva *et al.*, 2010; Parsons *et al.*, 2010). Integrins help cells resist mechanical force by assembling a large protein complex that connects to the cytoskeleton and forms a robust cytoskeletal meshwork that provides tensegrity, tensional integrity (Ingber, 2008; Geiger *et al.*, 2009; Humphrey *et al.*, 2014; Janostiak *et al.*, 2014). Integrins and their associated adhesion complexes act globally as a macromolecular mechanosensory complex and orchestrate a cellular response when force is applied to a tissue (Geiger *et al.*, 2009; Janostiak *et al.*, 2014). Integrins are believed to mediate mechanosensing via conformational changes that occur as a result of the pulling forces imposed upon binding to ECM ligands (Friedland *et al.*, 2009; Chen *et al.*, 2012; Humphrey *et al.*, 2014). For example, exposure shear forces in endothelial cells result in integrin activation (Tzima *et al.*, 2001). These conformational changes, collectively known as integrin activation, increase the affinity of integrins for their ECM ligands and are associated with signaling responses inside the cell that reinforce integrin-based adhesions (Askari *et al.*, 2009; Geiger *et al.*, 2009).

Other components of the integrin adhesion complex, such as vinculin, Talin, p130cas, and  $\alpha$ -actinin, are also known to act as mechanosensors and/or transducers (Geiger *et al.*, 2009).

This article was published online ahead of print in MBoc in Press (<http://www.molbiolcell.org/cgi/doi/10.1091/mbc.E15-05-0304>) on October 7, 2015.

\*These authors contributed equally to this article.

Address correspondence to: Guy Tanentzapf ([tanentz@mail.ubc.ca](mailto:tanentz@mail.ubc.ca)).

Abbreviations used: DYN, dynasore; e15, embryonic stage 15; e16, embryonic stage 16; e17, embryonic stage 17; ECM, extracellular matrix; FAK, focal adhesion kinase; FRAP, fluorescence recovery after photobleaching; GFP, green fluorescent protein; IAC, intracellular adhesion complex; IBS, integrin-binding site; L1, larval stage 1; L3, larval stage 3; MTJ, myotendinous junction; PBS, phosphate-buffered saline; SEM, standard error of the mean; THATCH, Talin-HIP1/R/Sla2p actin-tethering C-terminal homology; WT, wild type.

© 2015 Hákonardóttir, López-Ceballos, *et al.* This article is distributed by The American Society for Cell Biology under license from the author(s). Two months after publication it is available to the public under an Attribution–Noncommercial–Share Alike 3.0 Unported Creative Commons License (<http://creativecommons.org/licenses/by-nc-sa/3.0>).

“ASCB®,” “The American Society for Cell Biology®,” and “Molecular Biology of the Cell®” are registered trademarks of The American Society for Cell Biology.

In addition, signaling adapters in the IAC, such as paxillin and focal adhesion kinase (FAK), also play important roles in mechanosensing. It has been shown that FAK becomes activated by mechanical force and is required to generate the traction required for cell migration (Wang *et al.*, 2001; Seong *et al.*, 2013). FAK transduces the mechanotransduction signaling cascade by phosphorylating paxillin (Pasapera *et al.*, 2010). Paxillin, in turn, is recruited and stabilized by mechanical force at adhesions (Schiller *et al.*, 2011). One of the best-characterized mechanosensory IAC components is the large cytoplasmic adapter protein Talin. Talin contains helical bundles that can be stretched and opened up by mechanical force, revealing protein–protein interaction domains that mediate linkage to actin and reinforce the adhesion complex (del Rio *et al.*, 2009; Geiger *et al.*, 2009; Goult *et al.*, 2013). Talin is an essential linker between integrins and the actin cytoskeleton, as it binds to the integrin cytoplasmic tail, as well as to actin and actin linker proteins (Horwitz *et al.*, 1986; Smith and McCann, 2007; McCann and Craig, 1999; Kanchanawong *et al.*, 2010). Talin is therefore centrally positioned in the adhesion complex and can sense mechanical force generated from inside or outside the cell (del Rio *et al.*, 2009; Geiger *et al.*, 2009; Humphrey *et al.*, 2014). Moreover, because Talin is required for integrin activation, it potentially provides a platform where mechanical inputs can be translated into signals that modulate the stability and size of the adhesion complex. This hypothesis is reinforced by *in vivo* studies showing that a Talin mutant that cannot activate integrin fails to reinforce adhesion in response to increased force (Tadokoro *et al.*, 2003; Tanentzapf and Brown, 2006).

Coping with ongoing biomechanical strain is particularly important in muscles, as their main function is to generate and transduce force. Muscles generate force using a contractile cytoskeletal machinery called the sarcomere. Force is transmitted from sarcomeres to the rest of the body through specialized structures known as myotendinous junctions (MTJs). MTJs are specifically designed to withstand repeated exposure to large-scale mechanical force, and this is mainly achieved through integrin-based adhesions that form and maintain attachment between muscles and tendon cells (Bokel and Brown, 2002; Charvet *et al.*, 2013; Maartens and Brown, 2015). *Drosophila* MTJs have proven a useful and powerful model for studying muscle development, maintenance, and function (Maartens and Brown, 2015). Genetic screens in the fly have identified many conserved components of integrin-based adhesion that are essential for MTJ formation and maintenance (Maartens and Brown, 2015). Fly MTJs are a superb model in which to analyze integrin-based adhesion for several reasons. First, fly MTJs are large, discrete structures, which can be easily identified and analyzed (Bokel and Brown, 2002; Maartens and Brown, 2015). Second, because fly MTJs are located on the surface of fly embryos and larvae, they are well suited for imaging and, in particular, for live-imaging studies (Maartens and Brown, 2015). Third, the molecular components of integrin-based adhesion in MTJs are highly conserved with those found in vertebrate focal adhesions. Fourth, studies over the last two decades have generated a substantial array of tools and reagents with which to analyze fly MTJs.

The utility of the fly MTJs as a model system to study integrin-mediated adhesion is exemplified by the detailed structure–function work carried out in flies on integrin (Pines *et al.*, 2011, 2012), as well as on IAC components such as Talin (Liu *et al.*, 2000; Zervas *et al.*, 2001; Franco-Cea *et al.*, 2010). Based on information from biochemical studies, mutations were generated in fly integrin that interfered with binding to its ECM ligands, IAC components such as Talin and kindlin, and integrin activation (Pines *et al.*, 2011). Moreover, mutations were generated in fly Talin that impinged on its

ability to bind actin (Franco-Cea *et al.*, 2010), bind to integrin through either of its two integrin-binding sites, IBS-1 (Tanentzapf *et al.*, 2006) and IBS-2 (Ellis *et al.*, 2011), and support integrin activation (Ellis *et al.*, 2014). Comprehensive analysis of developmental and cell biological phenotypes in flies containing these mutant version of integrin and IAC components has provided useful mechanistic insights into the function and regulation of cell–ECM adhesion *in vivo* (Tanentzapf and Brown, 2006; Tanentzapf *et al.*, 2006; Franco-Cea *et al.*, 2010; Ellis *et al.*, 2011, 2014; Pines *et al.*, 2011).

The fly MTJs are an excellent model with which to study turnover of integrin adhesions in live, intact animals using fluorescence recovery after photobleaching (FRAP; Yuan *et al.*, 2010). This system is made even more versatile by the ability to manipulate the force acting on MTJs, using inducible mutations that relax or hypercontract muscles, while simultaneously studying IAC turnover with FRAP (Pines *et al.*, 2012). When combined with mathematical modeling, it has been possible to derive detailed mechanistic insight into the specific rate constants that underlie the delivery and removal of integrins from the membrane. This analysis showed that integrin activation plays a key role in force sensing by regulating the removal, or endocytosis, of integrins from the membrane (Pines *et al.*, 2012). Because previous work on adhesion turnover in fly MTJs focused on integrin themselves, less is known in the whole-animal context about the turnover of intracellular components of the adhesion complex. It has long been known in culture that modulating the force that acts on focal adhesions regulates their assembly and disassembly (Geiger *et al.*, 2001; Roca-Cusachs *et al.*, 2012). Several elegant cell culture studies analyzed the turnover of components of the integrin adhesion complex upon modulation of the actomyosin contractility and consequently mechanical force in cells in culture (Wolfenson *et al.*, 2011; Lavelin *et al.*, 2013). We therefore used the tools and approaches developed to study integrin turnover to study the turnover of the IAC component Talin under conditions of increased and reduced mechanical force.

Here we used FRAP and simple mathematical models to analyze the turnover of wild-type (WT) and mutant versions of Talin in response to force. These experiments were carried out in the fly MTJ in live, intact embryos and larvae using temperature-sensitive mutations to alter the amount of mechanical force placed on the MTJs. Our data show that the responses to either increased or decreased force are mediated by distinct mechanisms and thus reveal the strategies used during development to stabilize cell–ECM in order to maintain tissue architecture.

## RESULTS

### Development of a mathematical model and a modified FRAP approach to study Talin turnover

We previously described an analysis of integrin turnover in cells exposed to different levels of mechanical force (Pines *et al.*, 2012). This work relied on FRAP experiments, which, in combination with data fitting to a mathematical model, allowed the derivation of the two kinetic parameters that described integrin turnover: the rate constant for the exocytosis, or delivery, of integrins to the membrane ( $K_{\text{exo}}$ ) and the rate constant for the endocytosis, or removal, of integrins from the membrane ( $K_{\text{endo}}$ ). To use a similar approach to study the turnover of the intracellular adhesion complex, we established a new mathematical model. The IAC component Talin was chosen as the focus of these studies for a number of reasons: first, loss of Talin in flies fully recapitulates the phenotype obtained by loss of integrins, implying that Talin is essential for integrin function, which is not the case for other components of the IAC in flies (Brown *et al.*, 2002; Tanentzapf and Brown, 2006). Second, Talin has been extensively

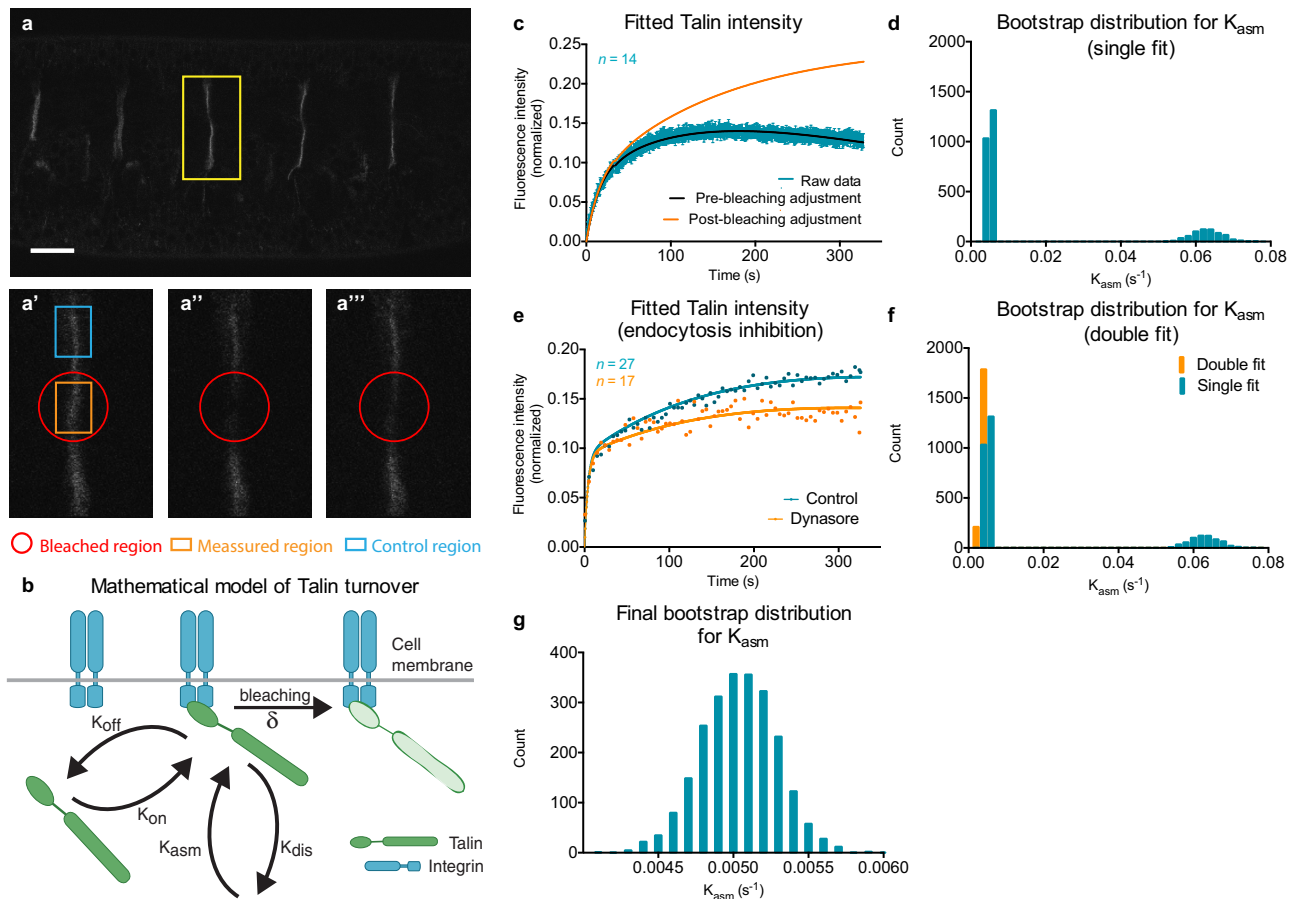


**FIGURE 1:** FRAP protocol and mathematical model to describe Talin turnover. (a) Example of embryonic MTJs in a Talin-GFP-tagged embryo in vivo (a'–a''') Representative images of a FRAP experiment, showing (a') the initial conditions, (a'') the bleaching event, and (a''') recovery over time. (b) Mathematical model that describes Talin kinetics using four parameters:  $K_{on}$  and  $K_{off}$  to measure the rate of free cytoplasmic Talin binding and unbinding at existing adhesion site, respectively, and  $K_{asm}$  and  $K_{dis}$  to measure the rate of complexed Talin assembly and disassembly at the membrane, respectively.  $\delta$ , photobleaching rate. (c) Recovery curve of raw data for WT-Talin-GFP at 25°C, fit adjustment and photobleaching adjustment derived from the mathematical model. (d) Simple fit bootstrap distribution for  $K_{asm}$  shows two possible solutions to the model. (e) Endocytosis inhibition using the chemical inhibitor Dynasore decreases Talin turnover. (f) Bootstrap distributions for a double fit between normal data sets and endocytosis inhibition data sets. The symmetry between  $K_{on}$ - $K_{asm}$  and  $K_{off}$ - $K_{dis}$  is broken by performing a double fit assuming  $K_{dis}$  is reduced. (g) Final bootstrap distribution for  $K_{asm}$ . Scale bar, 5  $\mu$ m.

studied in flies, and a large collection of tagged wild-type and mutant versions of Talin is available for use (Tanentzapf and Brown, 2006; Franco-Cea *et al.*, 2010; Ellis *et al.*, 2011, 2013, 2014). Third, Talin is a mechanosensory protein (del Rio *et al.*, 2009), and its ability to sense and respond to force means that it is likely to play key roles in mechanotransduction through integrin-based adhesions. Fourth, Talin mediates integrin activation, a key mechanism for regulating integrin adhesions in response to force (Calderwood *et al.*, 1999). The FRAP analysis used a tagged genomic rescue construct, Talin–green fluorescent protein (GFP), which was shown to fully rescue the embryonic and larval Talin loss-of-function phenotype and fully reproduce the expression of endogenous Talin (Tanentzapf and Brown, 2006; Franco-Cea *et al.*, 2010; Ellis *et al.*, 2011, 2013, 2014). Talin-GFP is robustly expressed and has previously proven suitable for FRAP studies (Yuan *et al.*, 2010; Bouaouina *et al.*, 2012; Ellis *et al.*, 2014).

A new mathematical model for turnover of IAC components was developed (Figure 1, a–c, and Supplemental Figure S3; see the Supplemental Material). The model assumes that the recruitment of Talin to the membrane occurs due to two simultaneous processes:

the first is the delivery of integrins and Talin to the membrane, forming a new adhesion complex that includes Talin as a core component; the rate constant that describes this process was therefore called  $K(\text{assembly})$  or  $K_{asm}$ . Second, once a complex is assembled in the membrane, additional Talin can simply bind to the adhesion complex by interacting with any of its many known binding partners, by a rate constant we call  $K_{on}$ . Next the model also assumes that the loss of Talin from the membrane occurs due to two simultaneous processes: the first is the unbinding of Talin from any of its binding partners from the adhesion complex, which itself remains intact; we call this rate constant  $K_{off}$ . The second is the disassembly of the adhesion complex, as well as the internalization of integrins and other components; this rate constant is  $K(\text{disassembly})$  or  $K_{dis}$ . Talin turnover is therefore controlled by four parameters:  $K_{on}$ ,  $K_{off}$ ,  $K_{dis}$ , and  $K_{asm}$ .

Use of this new mathematical model required adjustments to the protocol previously used to analyze integrin turnover (Pines *et al.*, 2012). First, because the new model has two additional parameters that must be fitted, a greater amount of information must be collected in each experiment. This was accomplished in the FRAP

protocol by increasing the rate of image acquisition. The new protocol gathered approximately eight times more data points per experiment than the previous protocol (see *Materials and Methods*). When using the new protocol we observed a slight increase in overall levels of photobleaching due to the higher rate of scanning. FRAP curves shown have not been corrected for photobleaching; however, the data derived from the model (rate constants) were adjusted to include the effect of photobleaching (see *Materials and Methods*). Second, when FRAP experiments were fitted to the model to obtain the four rate constants (Figure 1, c and d), often there was more than one solution. This was because the model has a fundamental symmetry: without additional information, it is impossible to distinguish the association/dissociation pathway from the assembly/disassembly pathway (Figure 1b). This meant there were two symmetric sets of possible rate constants that allow the model to fit the graph. To overcome this challenge, we developed a “double-fitting” protocol (Figure 1, d–f, and Supplemental Figure S1; see the Supplemental Material). For each experimental construct, we fitted the FRAP data to the model, thus obtaining two (symmetric) sets of rate constants describing the Talin turnover dynamics. Next we repeated the FRAP experiments in the presence of an inhibitor of endocytosis and fitted these data simultaneously with the unperturbed experiment under the assumption that only the rate constant for IAC disassembly ( $K_{\text{dis}}$ ) would vary between the two conditions. This second experiment breaks the symmetry inherent in the model and allows us to obtain a single-valued estimate for each rate constant (Figure 1g). This technique proved highly efficient and informative (Figure 1, d–f) and was carried out for each of the wild-type and mutant Talin transgenes. The inhibition protocol relies on previous studies showing that the disassembly of integrin-based adhesions requires endocytosis of integrins (Ezratty *et al.*, 2005, 2009; Pines *et al.*, 2012; Yuan *et al.*, 2010). This meant that suppressing  $K_{\text{dis}}$  could be accomplished by blocking endocytosis. To block endocytosis, a protocol was used to introduce the chemical inhibitor Dynasore into live fly embryos (Schulman *et al.*, 2013). The combination of the new model, improved time-resolution FRAP protocol, and double-fitting technique allowed us determine  $K_{\text{on}}$ ,  $K_{\text{off}}$ ,  $K_{\text{dis}}$ , and  $K_{\text{asm}}$  for each set of FRAP experiments.

### Analyzing the turnover of Talin under increased force

As previously shown, the amount of force that acts on integrin-based adhesion in the MTJ can be increased in an inducible manner using the temperature-sensitive mutation *Brkd*<sup>J29</sup> (Montana and Littleton, 2004; Pines *et al.*, 2012). Under wild-type conditions, beginning at early stage 16, muscles begin to undergo contractions that apply mechanical force on the MTJs (Crisp *et al.*, 2008). However, induction of *Brkd*<sup>J29</sup> significantly increases both the amplitude frequency of muscle contractions and magnitude of the force generation compared with wild type (Pines *et al.*, 2012). Using an established temperature-shift protocol (Pines *et al.*, 2012; see *Materials and Methods*), we exposed MTJs in stage 17 embryos containing the *Brkd*<sup>J29</sup> mutation to increased force and analyzed Talin turnover using FRAP. In line with previous observations, the shift from 25°C to the nonpermissive temperature of 37°C did not affect the mobile fraction of WT-Talin-GFP in control embryos (Figure 2, a and a'). In comparison, the application of force on the MTJs after a temperature shift led to a substantial, nearly 50% reduction in the Talin mobile fraction (Figure 2, b and b'). This indicates that Talin is stabilized at the membrane in response to the application of additional force on the adhesion complex.

Next we applied the “double-fitting” protocol to WT-Talin-GFP and determined the rate constants  $K_{\text{on}}$ ,  $K_{\text{off}}$ ,  $K_{\text{dis}}$ , and  $K_{\text{asm}}$ . Similar

to previous observations of integrin, the temperature shift by itself affected the rate constants, probably due to a change in metabolic rates (Figure 2a'). Moreover, the value of  $K_{\text{asm}}$  at 25°C was somewhat higher in the *Brkd*<sup>J29</sup> mutant, likely due to the different genetic background and perhaps the possibility that even at the permissive temperature, the *Brkd*<sup>J29</sup> phenotype was manifested slightly. Of importance, the shift to the higher temperature in the *Brkd*<sup>J29</sup> mutant background affected some rate constants very differently compared with the wild-type control, indicating a robust and specific mutant phenotype (Figure 2, b'' and c). Specifically, whereas in both the wild-type controls and *Brkd*<sup>J29</sup> mutants the temperature shift resulted in an increase in  $K_{\text{on}}$  and  $K_{\text{off}}$  and a slight decrease in  $K_{\text{dis}}$ ,  $K_{\text{asm}}$  was affected differently in controls versus mutant. In wild-type controls,  $K_{\text{asm}}$  decreased by 14% upon temperature shift, but it increased by 263% in the *Brkd*<sup>J29</sup> mutants (Figure 2, b'', c, and c'). To explore the effects of this shift on turnover, we calculated the ratio of the rate of adhesion complex assembly to disassembly (Figure 2d). Whereas in controls this ratio remained fairly constant at higher temperature (3.88 vs. 3.84 in 25 vs. 37°C, respectively) it increased nearly sevenfold in the induced *Brkd*<sup>J29</sup> mutants (1.28 vs. 8.32 in 25 vs. 37°C, respectively), consistent with a large shift toward a higher rate of adhesion complex assembly (Figure 2d). In comparison, the ratios of the rate of Talin binding on and off the assembled adhesion complex ( $K_{\text{on}}/K_{\text{off}}$ ) were not substantially different at 25 vs. 37°C between the control and *Brkd*<sup>J29</sup> mutant (Figure 2, c and d). Overall these data suggest that the main way in which Talin becomes stabilized in response to force is through an increased rate of assembly of the adhesion complex.

### Resolving the mechanism by which the turnover of Talin is regulated by increased force

To gain mechanistic insight into what regulates the rate of assembly of the integrin adhesion complex in response to force, we used a well-characterized collection of targeted mutations in Talin that have been generated and analyzed in our lab (Franco-Cea *et al.*, 2010; Ellis *et al.*, 2011, 2014). The effects of the *Brkd*<sup>J29</sup> mutation on the overall mobile fraction and the rate constants were analyzed in a background of Talin mutations that impinge on key aspects of Talin function (Figure 3). Talin mediates three main functions: regulating integrin activity, helping assemble and maintain the integrin adhesion complex, and binding to actin. Mutations were chosen that interfered with each of these processes. One of the main ways Talin is believed to modulate the stability of integrin-based adhesion is by regulating integrins through “inside-out” activation (Calderwood *et al.*, 1999). A mutation (TalinL334R; Ellis *et al.*, 2014) that specifically blocks “inside-out” activation was previously introduced into a GFP-tagged genomic rescue construct for Talin. GFP-tagged rescue transgenes were also generated that contain point mutations that block the two integrin-binding sites of Talin, IBS-1 (TalinR367A; Tanentzapf *et al.*, 2006) and IBS-2 (TalinK2094D/S2098D; Ellis *et al.*, 2011). The binding of Talin to integrin through IBS-1 is implicated in inside-out activation, whereas binding through IBS-2 is required to maintain the linkage of the IAC to integrin (Tanentzapf *et al.*, 2006; Ellis *et al.*, 2011). Finally, a GFP-tagged transgene was also made containing a mutation in Talin that blocks the ability of its C-terminal THATCH domain to bind actin and link the cytoskeleton to integrin (K2450D/V2451D/K2452D; Franco-Cea *et al.*, 2010). Of importance, in a heterozygous state such as that used in our experiments, none of these mutations affected muscle integrity.

Before analyzing the turnover of Talin transgenes containing point mutations, we confirmed that the temperature shift required to induce the *Brkd* mutation, from 25 to 37°C, did not affect the

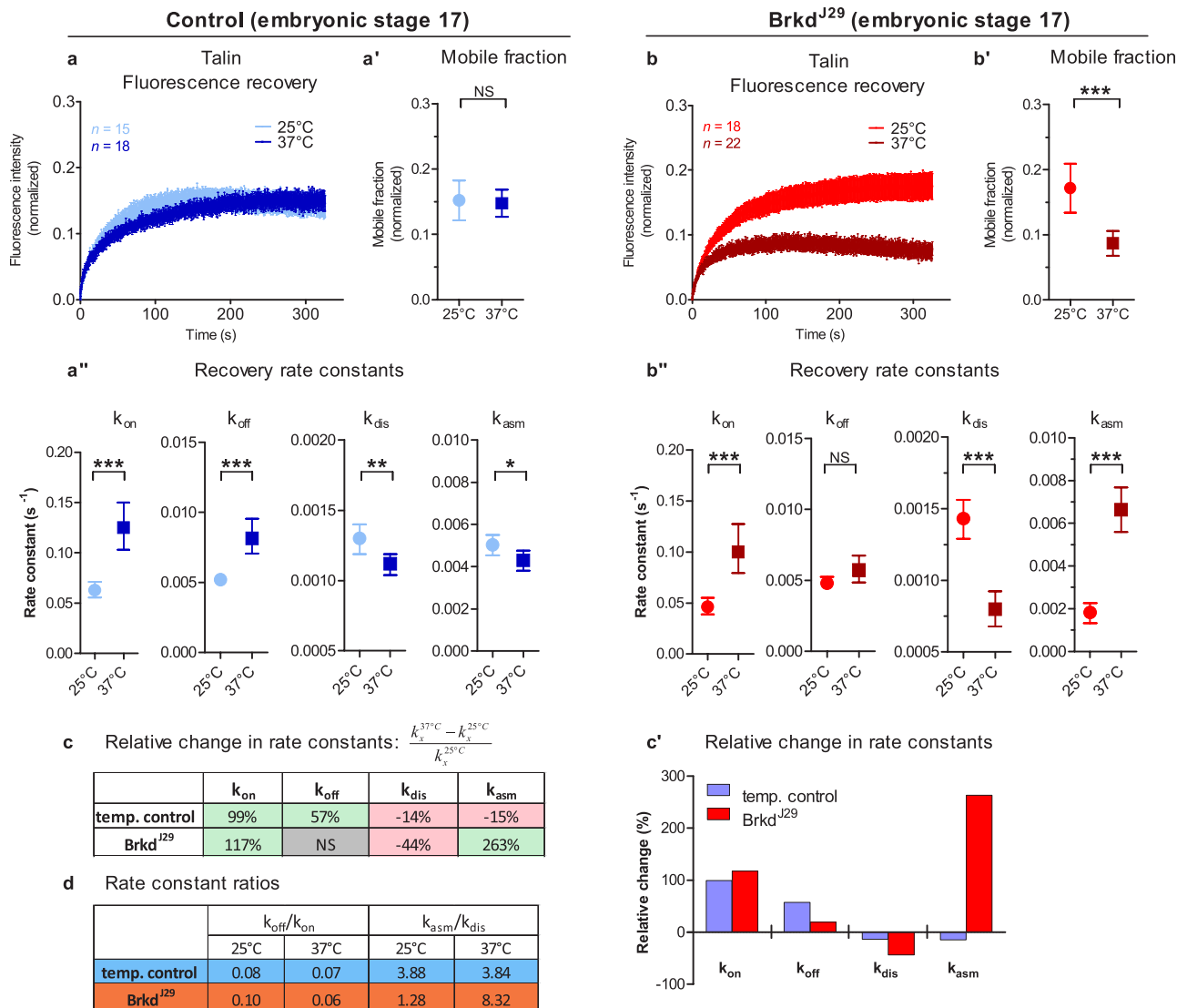


**FIGURE 2:** Increased mechanical force at MTJs stabilizes cell–ECM adhesion by regulating Talin turnover. FRAP analysis of stage 17 embryonic MTJs was performed to determine fluorescence recovery (a, b), final mobile fractions (a', b'), and rate constants  $K_{on}$ ,  $K_{off}$ ,  $K_{dis}$ , and  $K_{asm}$  (a'', b'') for WT-Talin-GFP (a) and WT-Talin-GFP in a *Brkd<sup>J29</sup>* background (b) at 25°C (light blue and red) and 37°C (dark blue and red). Relative change in rate constants (c, c') and rate constant ratios (d) at 25 and 37°C for wild-type controls and *Brkd<sup>J29</sup>* mutant flies. Each data point in a and b represents the mean value of on average 20 separate FRAP experiments; FRAP curves shown have not been corrected for photobleaching. Error bars are SEM. Error bars in a', a'', b', and b'' are 95% confidence intervals. ns indicates  $p > 0.05$ ; \* $p \leq 0.05$ , \*\* $p \leq 0.01$ , and \*\*\* $p \leq 0.001$ .

mobile fraction of the mutant Talin-GFP in control embryos (Supplemental Figure S2). Intriguingly, on their own, none of the Talin mutations studied completely blocked the typical reduction in turnover, manifested as a lower mobile fraction, caused by increasing the force acting on the MTJ (Figure 3). Nonetheless, mutations that disrupted Talin's ability to activate integrin, bind integrin through its IBS-2 domain, or bind actin via its C-terminal THATCH domain exhibited an attenuated response to the application of force on the MTJ, as judged by overall change in mobile fraction (Figure 3, b, d, and e, respectively). This shows that the mutations tested impinged on, but did not completely block, the ability of turnover to be modulated by increased force. In addition, we confirmed that simply increasing the temperature did not result in a statistically significant change in turnover for wild-type or mutant versions of Talin. To gain further insight into the effects of the Talin mutations, we used the

model fits to analyze changes in the reaction rates in response to increased force. Strikingly, we found that none of the Talin mutations tested exhibited the increase in  $K_{asm}$  that was observed for the WT-Talin-GFP upon induction of the *Brkd<sup>J29</sup>* mutation phenotype (Figure 3, summarized in f). Nonetheless, these mutations exhibited compensatory changes, such as a larger decrease in  $K_{off}$  compared with control, that explained their ability to partially modulate turnover in response to increased force (Figure 3, b–f). Analysis of the ratios of  $K_{off}/K_{on}$  and  $K_{asm}/K_{dis}$  in the Talin mutants provided further support for the hypothesis that they interfered with the response to increased force (Figure 3g). For example, upon application of higher force, all Talin mutants showed a smaller increase in  $K_{asm}/K_{dis}$  than controls (Figure 3g). This indicates that in the Talin mutants, adhesion assembly is not favored as it is in the wild type. Taken together, these results show that the stabilization



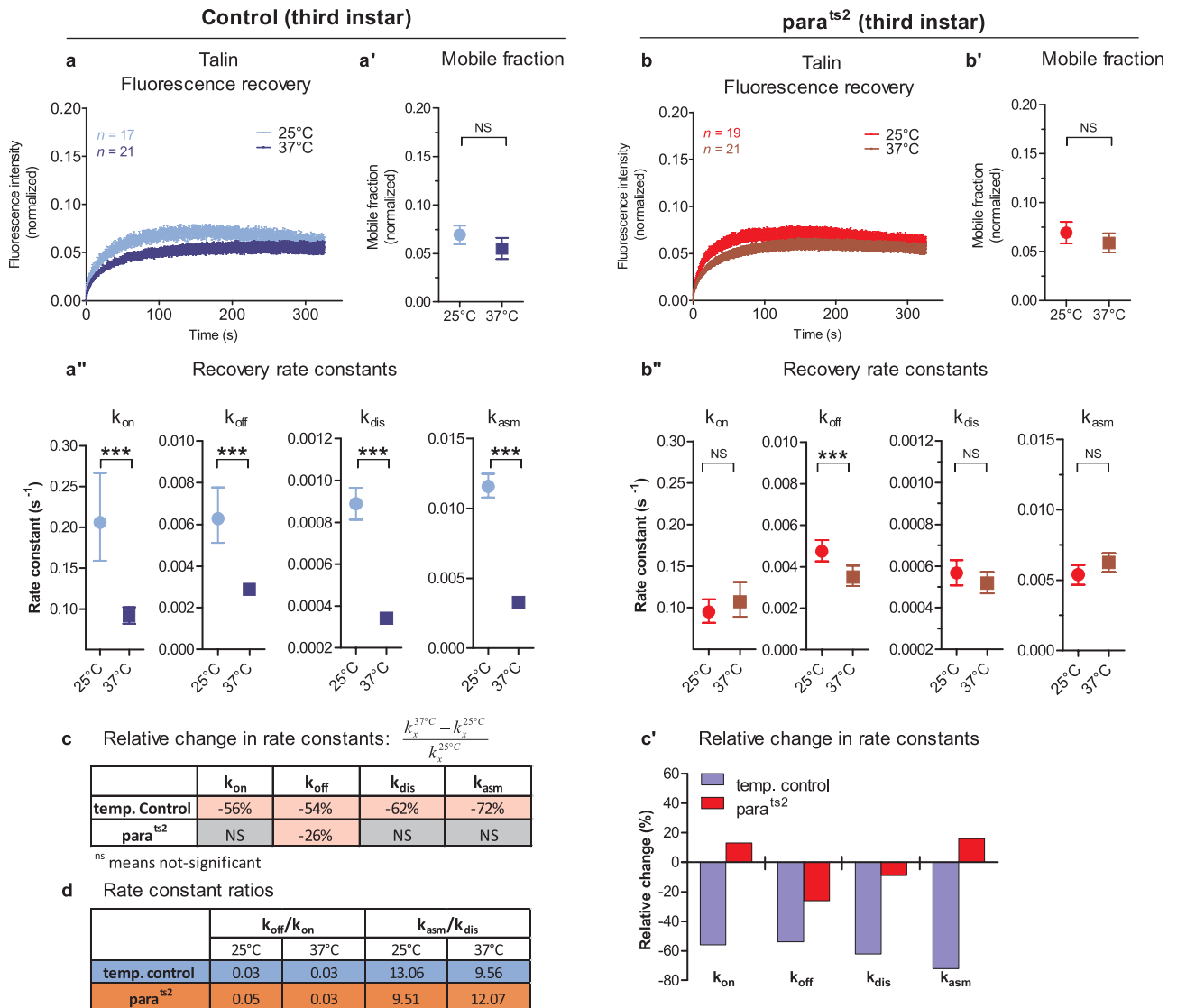


**FIGURE 4:** Decreased mechanical force at MTJs modifies Talin turnover. FRAP analysis of third-instar larval MTJs were performed to determine fluorescence recovery (a, b), final mobile fractions (a', b'), and rate constants  $K_{on}$ ,  $K_{off}$ ,  $K_{dis}$ , and  $K_{asm}$  (a'', b'') for WT-Talin-GFP (a) and WT-Talin-GFP in a *para<sup>ts2</sup>* background (b) at 25°C (light blue and red) and 37°C (dark blue and red). Relative change in rate constants (c, c') and rate constant ratios (d) at 25 and 37°C for wild-type controls and *para<sup>ts2</sup>* mutant flies. Each data point in a and b represents the mean value of on average 20 separate FRAP experiments; FRAP curves shown have not been corrected for photobleaching. Error bars are SEM. Error bars in a', a'', b', and b'' are 95% confidence intervals. ns indicates  $p > 0.05$ ; \*\*\* $p \leq 0.001$ .

of Talin in response to increased force is achieved by increasing the rate of assembly of new adhesions. Moreover, this increase in the rate of assembly is dependent on the ability of Talin to activate integrin, reinforce the adhesion complex, and link to actin. In the absence of these mechanisms, Talin can still be stabilized by other, compensatory mechanisms, such as by reducing its rate of unbinding from already assembled adhesion complexes. However, these compensatory mechanisms result in a less robust response to increased force.

#### Analyzing the turnover of Talin under decreased force

Next we characterized the turnover of the integrin adhesion complex at MTJs that experience reduced force compared with wild type. As we previously showed (Pines et al., 2012), the amount of force that acts on integrin-based adhesion in the MTJ can be decreased in an inducible manner using the temperature-sensitive

mutation *para<sup>ts2</sup>*. Induction of *para<sup>ts2</sup>* phenotype is known to significantly decrease the amplitude and frequency of muscle contractions, as well as the overall magnitude of the force generated by the muscle (Pines et al., 2012). The established temperature-shift protocol differed from that used for *Brkd<sup>J29</sup>*, as the effect is much weaker in embryos but becomes pronounced in larval stages (Pines et al., 2012). Thus all experiments employing *para<sup>ts2</sup>* were performed in third-instar larva. FRAP analysis was carried out using the WT-Talin-GFP in MTJs where the *para<sup>ts2</sup>* mutation was induced by transferring larva from the permissive (25°C) to the nonpermissive (37°C) temperature (Figure 4). No change in the mobile fraction of WT-Talin-GFP in was observed compared with control embryos upon induction of the *para<sup>ts2</sup>* phenotype (Figure 4, a, a', b, and b'). This was similar to what was previously observed for integrin upon induction of *para<sup>ts2</sup>* (Pines et al., 2012). However, despite the overall constant mobile fraction analysis, the parameter fits for the mathematical

model showed a uniform, across-the-board increase in all four rate constants (Figure 4, a–c). Specifically, whereas in control third-instar larva a shift to the 37°C causes an overall drop in the rate constants (Figure 4a’), this did not take place in the *para<sup>ts2</sup>* mutants (Figure 4b), representing a net increase in all rate constants compared with the control (Figure 4c). This suggests that even though the proportion of Talin that undergoes turnover remains the same, this pool undergoes more rapid turnover. Consistent with this hypothesis, analysis of the ratios  $K_{asm}/K_{dis}$  and  $K_{on}/K_{off}$  showed only minor differences between the control and *para<sup>ts2</sup>* larvae, which explains how increased rates of turnover can occur while the mobile fraction remains constant (Figure 4d). Taken together, these results show that reducing the force that acts on MTJ leads to a coordinated increase in the rate constants that govern Talin turnover, while the overall mobile fraction of Talin remains constant.

### Uncovering the mechanism by which the turnover of Talin is regulated by decreased force

Next we analyzed the effect of *para<sup>ts2</sup>* in a background of Talin mutations that interfered with inside-out activation, actin binding, and adhesion complex assembly. First, as before, we confirmed that simply increasing the temperature did not result in a statistically significant change in turnover for wild-type or mutant versions of Talin. Second, the force acting on MTJs was reduced by moving the flies to the nonpermissive temperature. On induction of the paralysis, the effects on mobile fraction were, as in the wild type, negligible for all Talin mutations, with the exception of the mutation in the C-terminal integrin-binding site (IBS-2), for which a small reduction in mobile fraction was seen (Figure 5, a–e). Analysis of the rate constants governing Talin turnover in mutant backgrounds revealed that mutations in the actin-binding domain or those that affect activation acted similarly to wild-type Talin (Figure 5f). One exception was the mutation in IBS-2 that affects adhesion complex assembly and stability (Ellis *et al.*, 2011; Figure 5, e and f). In the IBS-2 background, inducing the *para<sup>ts2</sup>* mutation led to a much larger increase in the rate constants, and these changes were not as evenly distributed as they are in the wild type. As a result, the ratio  $K_{asm}/K_{dis}$  nearly doubled upon induction of the *para<sup>ts2</sup>* phenotype; this increase in the overall assembly of adhesion explains the stabilization of adhesion manifest by the lower mobile fraction observed in the IBS-2 mutant. These results show that under conditions of reduced force, the coordinated increase in rate constants that allows turnover to increase but to maintain a stable pool of Talin at the membrane is dependent on the activity of the IBS-2 domain of Talin.

### Reducing FAK activity partially mimics the effect of increased force on Talin turnover

FAK is a key regulator of integrin turnover in response to force (Wang *et al.*, 2001; Pasapera *et al.*, 2010; Seong *et al.*, 2013). We therefore asked whether modulating FAK activity could reproduce some of the effects of increased force. To this end, we expressed a mutant version of FAK (Y430F; equivalent to the vertebrate Y397F mutation) that severely impairs the autophosphorylation site and consequently the ability of FAK to be activated (Grabbe *et al.*, 2004; Tsai *et al.*, 2008; Macagno *et al.*, 2014). We found that the expression of the FAK(Y430F) transgene resulted in a lower Talin mobile fraction, consistent with stabilization of Talin at MTJs (Figure 6). Analysis of the turnover rate constants revealed that modulating FAK activity had a statistically significant effect on some of the rate constants compared with the control (Figure 6a). Specifically, the expression of the FAK(Y430F) resulted in an increase in  $K_{on}$  and  $K_{asm}$  and a slight decrease in  $K_{dis}$ . Specifically,  $K_{dis}$  decreased by 32%

upon expression of the FAK(Y430F) transgene, whereas  $K_{on}$  and  $K_{asm}$  increased by 150 and 27%, respectively (Figure 6b). To explore the effects of these changes in the rate constants on turnover, we calculated the ratio of the rate of adhesion complex assembly to disassembly ( $K_{asm}/K_{dis}$ ) and found it to increase by 89%, from 5.6 to 10.6 (Figure 6c). In comparison, the ratio of the rate of Talin binding off and on for the assembled adhesion complex ( $K_{off}/K_{on}$ ) decreased by 42%, from 0.061 to 0.035 (Figure 6, b and c). Overall these data suggest that FAK is required to maintain the junction in a more dynamic state and that preventing FAK activation both promotes junction assembly and suppresses junction breakdown.

### Changes in rate constants underlie developmental regulation of Talin turnover

Over the course of development, integrin-based adhesions at the MTJs become increasingly stable as the mobile fraction of integrin and IAC components, including Talin, tensin, and ILK, decreases (Figure 7, a and b; Yuan *et al.*, 2010; Pines *et al.*, 2012). Reduced turnover can assist in the reinforcement and the buildup of Talin at the MTJs that occurs as development progress (Devenport *et al.*, 2007; Yuan *et al.*, 2010). To determine the mechanism underlying this developmentally regulated stabilization of the IAC at MTJs, we carried out a series of FRAP experiments with Talin-GFP, starting at embryonic stages 15–17 and then in first- and third-instar larvae. As before, FRAP data were analyzed by fitting to the mathematical model (Figure 7). This analysis identified two different mechanisms that mediated the stabilization of junctions in the embryo, as well a third, separate mechanism that operated in larva. The first embryonic mechanism was responsible for the large decline in turnover during the transition from stage 15 to stage 16 in embryogenesis, which is the time when muscle contractility begins. During this transition, all of the rate constants,  $K_{off}$ ,  $K_{on}$ ,  $K_{asm}$ , and  $K_{dis}$ , declined. The second embryonic mechanism was responsible for reducing turnover during the transition from stage 16 to stage 17, which is the time when muscle contractility gains in strength. During this transition, the rates of adhesion complex disassembly,  $K_{dis}$ , and of Talin binding off of the adhesion complex,  $K_{off}$ , declined substantially (Figure 7, d and e). The third, larval mechanism was responsible for the moderate decrease in turnover that occurs over larval life, which is a time when muscles undergo massive growth. During this transition, there was a notable increase in the rate of Talin binding to already assembled adhesion complexes,  $K_{on}$ , and a smaller increase in the rate of assembly of new adhesion,  $K_{asm}$  (Figure 7, c and f). Therefore we conclude that the stabilization of cell–ECM adhesions at the MTJs is accomplished by stage-specific modulation of the different processes that mediate junctional turnover. Although initially, when muscles begin to contract, adhesions are stabilized by an across-the-board reduction in rate constants, in later embryonic stages, the rates of both adhesion complex disassembly and unbinding of Talin from the assembled complex decline. In contrast, in larval stages, the stabilization of cell–ECM adhesions at the MTJs is accomplished largely by increasing the binding rate of Talin to the assembled adhesion complex.

## DISCUSSION

In this work, we used a quantitative *in vivo* approach to study the turnover of the IAC component Talin in response to modulation of the force acting upon integrin-based adhesions. Our analysis identified the different strategies used to modulate the stability of integrin-based adhesion in response to the application of increased and decreased force, as well as during tissue stabilization after embryonic development. The experiments described here relied on imaging

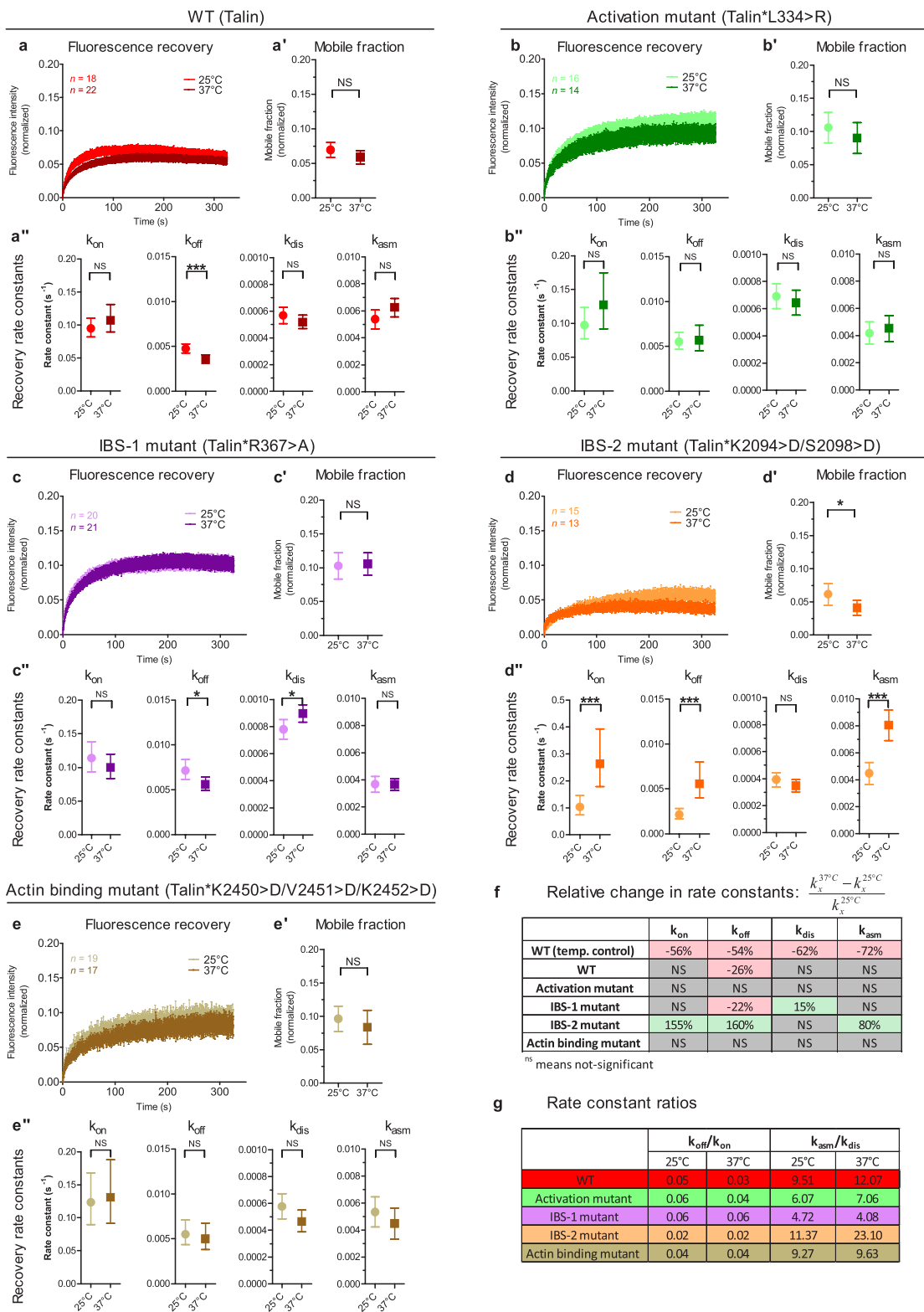


**FIGURE 5:** The Talin IBS-2 domain is essential to coordinate turnover in response to reduced mechanical force. FRAP analysis of third-instar larval MTJs determines fluorescence recovery (a–e), final mobile fractions (a’–e’), and rate constants  $k_{on}$ ,  $k_{off}$ ,  $k_{dis}$ , and  $k_{asm}$  (a’’–e’’) for wild-type and mutant versions of GFP-tagged Talin at 25°C (light colors) and 37°C (dark colors) in a wild-type and a *para<sup>ts2</sup>* background. Relative change in rate constants (f) and rate constant ratios (g) at 25 and 37°C for wild-type and mutant versions of Talin-GFP in wild-type and *para<sup>ts2</sup>* backgrounds. Each data point in a–e represents the mean value of on average 20 separate FRAP experiments; FRAP curves shown have not been corrected for photobleaching. Error bars are SEM. Error bars in a’–e’ and a’’–e’’ are 95% confidence intervals. ns indicates  $p > 0.05$ ; \* $p \leq 0.05$  and \*\*\* $p \leq 0.001$ .

## FAK-Y430F (embryonic stage 17)

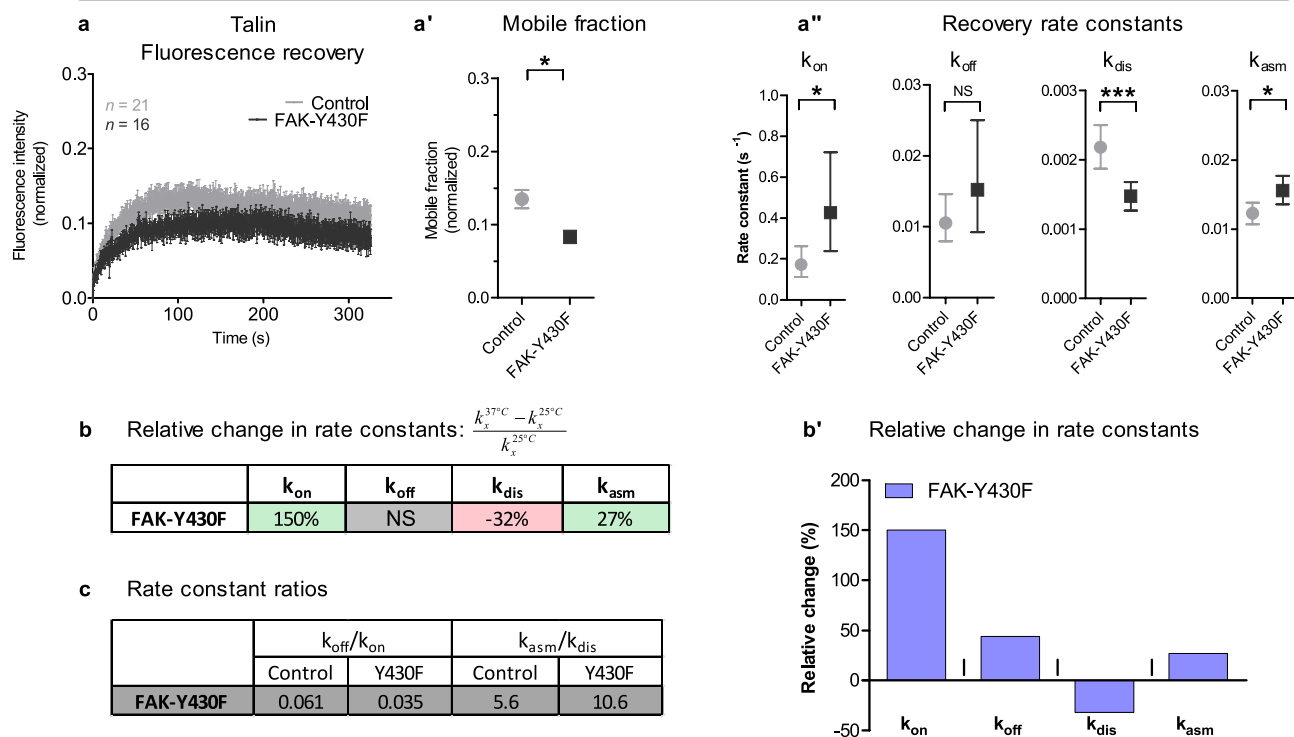


**FIGURE 6:** Reduced FAK activity affects integrin turnover in a manner similar to increased force. FRAP analysis of stage 17 embryonic MTJs were performed to analyze turnover of Talin-GFP in control (Mef2-GAL4/+ ) flies vs. flies expressing the nonactivatable FAK-Y430F mutant (a), final mobile fractions (a'), and rate constants  $k_{\text{on}}$ ,  $k_{\text{off}}$ ,  $k_{\text{dis}}$ , and  $k_{\text{asm}}$  (a''). Relative change in rate constants (b, b') and rate constant ratios (c) from controls and FAK-Y430F-expressing flies. Each data point in a represents the mean value of on average 20 separate FRAP experiments; FRAP curves shown have not been corrected for photobleaching. Error bars are SEM. Error bars in a' and a'' are 95% confidence intervals. ns indicates  $p > 0.05$ ; \* $p \leq 0.05$  and \*\*\* $p \leq 0.001$ .

and genetic tools that were previously developed to study the turnover of integrin adhesion receptors (Yuan *et al.*, 2010; Pines *et al.*, 2012). However, adapting these tools to analyze Talin turnover proved technically challenging. Modeling the turnover of intracellular adhesion components is inherently more complicated than modeling the turnover of transmembrane adhesion receptors, as it involves a greater number of variables. Specifically, there are multiple ways for intracellular adhesion complex components to be recruited to and be removed from sites of adhesion. Nonetheless, we were able to overcome these challenges by enhancing the resolution of our data collection technique and introducing a novel two-step “double-fitting” strategy based on a well-characterized pharmacological perturbation. This approach is powerful and versatile. We believe that it can be customized and applied to efforts to model the turnover of other membrane-bound complexes using FRAP. Moreover, the tools and mathematical model used to analyze Talin turnover can be adapted to study the turnover of other components of the integrin adhesion complex in the fly MTJs.

One of our most striking results was the strong increase in the rate of assembly of new adhesions when higher force was applied to MTJs. The resulting effect of this, a nearly sevenfold increase in the ratio of assembly to disassembly of adhesions, provides an elegant and powerful method to quickly reinforce and stabilize adhesions. A number of mechanisms could be responsible for this increased rate of assembly. First, it is known that the application of mechanical force activates integrins and can lead to increased assembly and reinforcement of new adhesions (Puklin-Faucher and Sheetz, 2009).

Consistent with this hypothesis, we find that mutations in Talin that disrupt integrin activation did not exhibit an increased rate of assembly of new adhesions when higher force was applied to the MTJs. Second, it is known that the application of mechanical force to adhesion complex components such as Talin and vinculin leads to stretching and conformational changes that reveal protein–protein interaction modules and phosphorylation sites (Sawada *et al.*, Cell 2006; del Rio *et al.*, 2009; Dumbauld *et al.*, 2013; Goult *et al.*, 2013). Based on these findings, it has been hypothesized that the application of force leads to the recruitment of additional components to adhesions and consequently to adhesion maturation and reinforcement (del Rio *et al.*, 2009; Lavelin *et al.*, 2013). Consistent with this hypothesis, we find that mutations in the actin-binding domain of Talin, which interfere with anchorage to the cytoskeleton required for stretching of Talin, also fail to up-regulate adhesion assembly in response to higher force. Third, it is possible the modulation of force affects the endocytosis and exocytosis of other components of the integrin adhesion complex. Finally, we find evidence that modulation of FAK activation, which is believed to be part of the cascade that controls junction turnover in response to force in cell culture, might contribute to the stabilization of junctions exposed to mechanical force in flies. Expression of a mutant version of FAK that cannot be activated by phosphorylation affects turnover in a manner reminiscent to the application of mechanical force.

Overall our new data showing higher rate of adhesion complex assembly in response to increased force are very much in line with our previous work showing that the application of more force on

## WT Talin in development (heterozygous background)

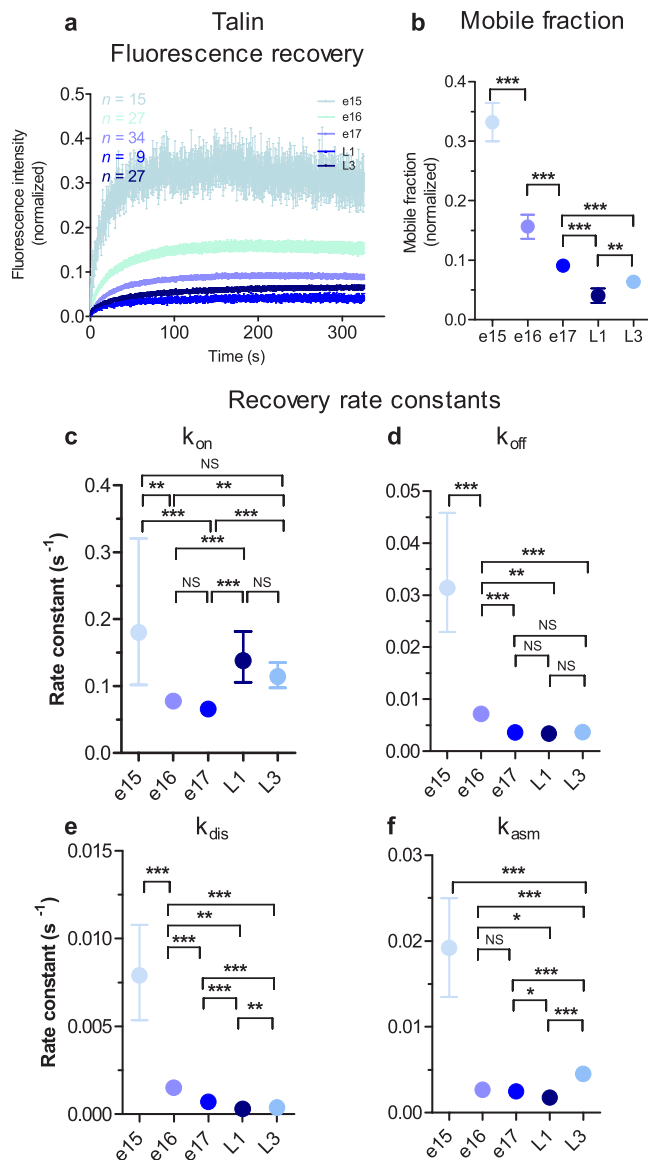


**FIGURE 7:** Talin turnover is developmentally regulated through distinct mechanisms. (a) FRAP analysis of WT-Talin-GFP at progressive developmental stages: embryonic stages 15 (e15), 16 (e16), and 17 (e17) and first (L1) and third (L3) larval instars. (b) Mobile fraction for Talin-GFP at progressive developmental stages. Rate constants  $K_{on}$  (c),  $K_{off}$  (d),  $K_{dis}$  (e), and  $K_{asm}$  (f) for Talin-GFP at progressive developmental stages. These experiments were conducted using a copy of the Talin-GFP transgene in a heterozygous null mutant of the Talin gene (*rhea<sup>2/2</sup>*). Each data point in a represents the mean value of on average 20 separate FRAP experiments; FRAP curves shown have not been corrected for photobleaching. Error bars are SEM. Error bars in b are 95% confidence intervals. ns indicates  $p > 0.05$ ; \* $p \leq 0.05$ , \*\* $p \leq 0.01$ , and \*\*\* $p \leq 0.001$ .

MTJs correlates with increased availability of integrins at the membrane (Pines et al., 2012). When mechanical force is increased, the rate of removal of integrins from the membrane is substantially reduced, which results in stabilization of integrins at the membrane (Pines et al., 2012). These results fit well with experiments on

micropatterned slides that suggested that focal adhesion growth is regulated by the balance between intracellular and extracellular forces acting on integrins (Gallant et al., 2005; Coyer et al., 2012). According to models put forth based on these cell culture experiments, increasing extracellular, externally applied force would lead to assembly of more adhesions; this is very much in agreement with our in vivo results.

The effects on Talin turnover of reducing the force that acted on integrin-based adhesions at the MTJs were complex. The mobile fraction remained constant, indicating that the proportion of Talin undergoing turnover was not greatly changed. However, the overall rates of turnover of this mobile pool were significantly higher. These results bear striking resemblance to the behavior of integrin turnover under reduced force, as the mobile fraction of integrins also remained unchanged, but turnover rates were higher in response to the reduced mechanical load (Pines et al., 2012). It is thus likely that a similar strategy is used by both integrins and the intracellular adhesion complex to maintain stable adhesion in MTJs that experience a reduction in force. We previously speculated that this strategy was used because it allows greater flexibility during turnover without compromising the stability of these structures, as a similar proportion of IAC components undergoes turnover, but this turnover happens faster (Pines et al., 2012). However, to ensure that increased turnover rates do not result in a higher mobile fraction, it is crucial to coordinate changes in the rate constants. Our mutational analysis identifies an important role for the second, C-terminal integrin-binding site in Talin, known as IBS-2, in coordinating such an increase. In an IBS-2 Talin mutant background, there is a failure to coordinate the increase in the rate constants, and as a result, the mobile fraction is slightly lower than with controls. This fits with our previous analysis, which identified IBS-2 as a key factor in regulating the assembly and reinforcement of integrin-based adhesions (Ellis et al., 2011). Moreover, these results are in line with analysis of the turnover of isolated domains of Talin in focal adhesions (Himmel et al., 2009). These cell culture FRAP studies found that the IBS-2 domain of Talin plays a critical role in regulating the kinetics and binding affinity of the Talin to its partners (Himmel et al., 2009). Of importance, it was found that the interaction of the IBS-2 domain with integrin was highly regulated by conformational changes of the kind induced by the application of mechanical force (Himmel et al., 2009). Taken together, our data show that the turnover of integrin adhesion complex components by force is bidirectional: more force inhibits turnover, and less force promotes turnover.

In line with this conclusion, our studies complement previous studies in cell culture that looked at the turnover of focal adhesion proteins upon inhibition of actomyosin-generated forces (Wolfenson et al., 2011; Lavelin et al., 2013). The approach of reducing actomyosin-generated forces for cells in culture is in principle similar to that of using the *para<sup>ts2</sup>* mutation in MTJs in vivo, although, of note, unlike MTJs, loss of contractile force leads to disassembly of focal adhesions (Wolfenson et al., 2011; Lavelin et al., 2013). In contrast to our work, the model used to study the inhibition of actomyosin-generated forces in culture was simpler and focused on the association and dissociation rate constants  $K_{on}$  and  $K_{off}$  of integrin adhesion complex components (Wolfenson et al., 2011; Lavelin et al., 2013). Overall the effect of reduced force on  $K_{on}/K_{off}$  varied considerably between the proteins (Wolfenson et al., 2011; Lavelin et al., 2013). The main general conclusion derived from these studies is that changes in  $K_{on}/K_{off}$  initiate focal adhesion disassembly by affecting the molecular turnover of focal adhesions and altering their composition (Wolfenson et al., 2011; Lavelin et al., 2013). A key difference between analysis of turnover in MTJs versus in culture is that MTJs

are stable, long-lasting adhesions, and it is crucial not to dismantle these junctions under reduced force. In comparison, the dynamic conditions experienced by cells in culture allow, and in many instances require, remodeling and breakdown of adhesions in response to reduced force. These results illustrate the need for diverse, context- and tissue-specific strategies to regulate adhesion stability in response to force-mediated cues.

An important advantage of using the MTJs as a model to study turnover is the ability to analyze adhesion turnover over the course of development. We hypothesized that in the course of fly development, greater force is applied on the MTJs and that this reinforces and stabilizes them. In particular, a force-mediated reduction in the turnover of Talin increases its availability at the membrane to bind to integrins in order to both activate and connect them to the cytoskeleton. During development, there are three main factors that affect the amount of force placed on the MTJs. First, at around stage 15, muscle contraction is initiated, and force begins to be applied on the MTJs (Crisp *et al.*, 2008). Second, the transition that occurs during the last stage of fly embryonic development, stage 17, involves the beginning of much stronger coordinated and uniform waves of muscle contraction associated with locomotion (Tanentzapf and Brown, 2006). Third, during larval growth, there is a tremendous expansion in muscle size and volume, and this places a great deal of additional mechanical stress on the MTJs (Yuan *et al.*, 2010). Corresponding to each of these three phases, we observe the initiation of a specific program that reduces the turnover of IAC components. First, we see a uniform, general, and significant reduction in all the rate constants as soon as force is any force is placed on integrin-based adhesions at the MTJ. Second, during the late embryonic stage, there is a marked decline in both rate of adhesion complex disassembly,  $K_{\text{dis}}$ , and the rate of Talin binding off of the adhesion complex,  $K_{\text{off}}$ . Third, during later larval stages, there is an increase in both the rate of adhesion complex assembly,  $K_{\text{asm}}$ , and the rate of Talin binding onto the adhesion complex,  $K_{\text{on}}$ . These are different strategies that target different aspects of the adhesion life cycle. Intriguingly, the larval mechanism relies only partially on changes in  $K_{\text{asm}}$ , whereas the late embryonic mechanism dispenses with any changes to  $K_{\text{asm}}$ . This is surprising because changes in  $K_{\text{asm}}$  appear to be the main method used by MTJs to respond to increased force, but this does not appear to be regulatory mechanism during all stages of development. These data suggest that regulation by mechanical force is perhaps not the only strategy used to modulate adhesion complex turnover during development. In this regard, our results are reminiscent of work in cell culture that identified mechanisms that promote maturation and reinforcement of adhesion across a range of tensions. These studies showed that the application of force by itself is not always sufficient for the maturation of focal adhesions (Stricker *et al.*, 2011; Oakes *et al.*, 2012; Oakes and Gardel, 2014). In fact, actin architecture is an important structure in regulating focal adhesion assembly (Oakes *et al.*, 2012; Oakes and Gardel, 2014). The developmental period we analyzed in this study corresponds to a time during which substantial actin remodeling occurs within the muscles. It is therefore likely that these global-level changes to the actin cytoskeleton provide an additional means, independently of tension, of regulating the maturation and stabilization of integrin-based adhesions at the MTJ.

On the basis of the results presented here, our previous observations, and work in vertebrate systems, we propose the following model for how force regulates adhesion complex turnover in fly MTJs *in vivo*. When increased mechanical force is applied on the MTJs, this initiates outside-in signaling through the integrin, which acts to decrease the rate of its internalization via endocytosis (Pines

*et al.*, 2012). As a result of reduced integrin internalization, there is increased availability of integrin at the membrane, a higher rate of adhesion complex assembly, and consequently reinforcement and stabilization of the adhesion complex. Reinforcement of the IAC also requires outside-in signaling and involves additional recruitment of components to the adhesion complex through conformational changes. When less mechanical force is applied on tissues, the overall pool of integrin and Talin that undergoes turnover remains unchanged, but the actual rates of turnover for the mobile pool are increased. This increase needs to be coordinated carefully or the mobile fraction could become misregulated, potentially leading to disruption of the MTJ; the C-terminal integrin-binding site 2 of Talin plays an important role in regulating turnover in response to decreased force (Pines *et al.*, 2012). Taken together, these mechanisms optimize tissue strength and stability under conditions of varying mechanical stress.

## MATERIALS AND METHODS

### Fly stocks

To visualize Talin *in vivo*, we used embryos expressing endogenous levels of nonlabeled Talin, as well as an additional copy of pUBI-Talin-GFP (Yuan *et al.*, 2010). For mutational analysis, we used pUBI-Talin(mutant)-GFP for the following: K2450D/V2451D/K245D (Franco-Cea *et al.*, 2010), K2094D/S2098D (Ellis *et al.*, 2011), R367A (Tanentzapf and Brown, 2006), and L334R (Ellis *et al.*, 2014). *Brkd<sup>J29</sup>/TM3* and *para<sup>ts2</sup>* were provided by J. Troy Littleton (MIT, Cambridge, MA) and are described elsewhere (Montana and Littleton, 2004). Fluorescent Talin transgenes in either a *Brkd<sup>J29</sup>* (embryonic stage 17) or *para<sup>ts2</sup>* (in males, as *para<sup>ts2</sup>* is on the X, of third-instar larvae, since the contractility phenotype manifests at this stage) heterozygous background were used to perform FRAP analysis by selecting against fluorescent balancers. To change FAK activity (Figure 6), we used an inactive version of FAK (UAS-FAK-Y430F) expressed in the muscle using *mef2GAL4* in combination with WT-Talin-GFP. For the developmental series (Figure 7), a copy of pUBI-Talin-GFP was expressed in a *rhea<sup>79</sup>* heterozygous mutant background. Animals with a copy of pUBI-Talin-GFP were used in endocytosis inhibition experiments.

### FRAP experiments

FRAP analysis was performed in whole-mount embryos (stages 16 and 17) and larvae (first and third instars) in phosphate-buffered saline (PBS) 1–1.5 h after mounting. Embryos were dechorionated in 50% bleach for 4 min, washed with water, and mounted in PBS on glass slides. Larvae were washed and mounted in the same conditions. FRAP analysis was carried out in a mixed population of MTJs as described in Pines *et al.* (2012). To modulate force, *Brkd<sup>J29</sup>* and *para<sup>ts2</sup>* animals were incubated at 37°C for 1–1.5 h after mounting. To maintain the temperature while imaging, a Tokai Hit stage-top incubator (Tokai Hit, Fujinomiya, Japan) was used. To conduct endocytosis inhibition, we used the *in vivo* permeabilization protocol described in Schulman *et al.* (2013) to deliver Dynasore (150 and 200  $\mu\text{M}$  in dimethyl sulfoxide; Sigma-Aldrich, St. Louis, MO) into the animals. As reported previously, the relatively short exposure time to Dynasore ensures no gross anomalies in muscle function and morphology (Pines *et al.*, 2012). After the drug treatment, no waiting period was needed before performing FRAP. FRAP was carried out on an inverted confocal microscope (Olympus FluoView, FV1000) with an UplanSApo60 $\times$ /1.35 oil objective (Olympus, Tokyo, Japan). Bleaching was performed with a 473-nm laser at 5% power using the Tornado scanning tool (Olympus) for 2 s at 100  $\mu\text{s}/\text{pixel}$ . Fluorescence intensity was recorded for 825 frames, every 0.4 s, of

which 75 frames were taken before the bleaching event. To control for sample movement in and out of focus, a region of interest was selected in nonbleached region. Only FRAP curves for which the fluorescence intensity remained steady throughout the whole experiment were used for analysis.

### Mathematical model and fitting

As described earlier, a three-compartment model of fluorescent Talin was developed as a system of ordinary differential equations (see the Supplemental Material). We fitted the parameters of this model to the FRAP recovery curves by minimizing the sum-of-square residuals between the model and the data. Confidence intervals on the parameters were estimated using bootstrapping (Efron and Tibshirani, 1993). A simple estimate of the mobile fraction was also made for each replicate as the recovery fraction of an exponential curve. This was done independently of the model fitting and photobleaching correction, and the mean is reported for each experimental condition.

### REFERENCES

- Askari JA, Buckley PA, Mould AP, Humphries MJ (2009). Linking integrin conformation to function. *J Cell Sci* 122, 165–170.
- Bokel C, Brown NH (2002). Integrins in development: moving on, responding to, and sticking to the extracellular matrix. *Dev Cell* 3, 311–321.
- Bouaouina M, Harburger DS, Calderwood DA (2012). Talin and signaling through integrins. *Methods Mol Biol* 757, 325–347.
- Brown NH, Gregory SL, Rickoll WL, Fessler LI, Prout M, White RA, Fristrom JW (2002). Talin is essential for integrin function in *Drosophila*. *Dev Cell* 3, 569–579.
- Calderwood DA, Zent R, Grant R, Rees DJ, Hynes RO, Ginsberg MH (1999). The Talin head domain binds to integrin beta subunit cytoplasmic tails and regulates integrin activation. *J Biol Chem* 274, 28071–28074.
- Charvet B, Guiraud A, Malbouyres M, Zwolanek D, Guillon E, Breaud S, Monnot C, Schulze J, Bader HL, Allard B, et al. (2013). Knockdown of col22a1 gene in zebrafish induces a muscular dystrophy by disruption of the myotendinous junction. *Development* 140, 4602–4613.
- Chen W, Lou J, Evans EA, Zhu C (2012). Observing force-regulated conformational changes and ligand dissociation from a single integrin on cells. *J Cell Biol* 199, 497–512.
- Coyer SR, Singh A, Dumbauld DW, Calderwood DA, Craig SW, Delamarche E, Garcia AJ (2012). Nanopatterning reveals an ECM area threshold for focal adhesion assembly and force transmission that is regulated by integrin activation and cytoskeleton tension. *J Cell Sci* 125, 5110–5123.
- Crisp S, Evers JF, Fiala A, Bate M (2008). The development of motor coordination in *Drosophila* embryos. *Development* 135, 3707–3717.
- del Rio A, Perez-Jimenez R, Liu R, Roca-Cusachs P, Fernandez JM, Sheetz MP (2009). Stretching single Talin rod molecules activates vinculin binding. *Science* 323, 638–641.
- Devenport D, Bunch TA, Bloor JW, Brower DL, Brown NH (2007). Mutations in the *Drosophila* alphaPS2 integrin subunit uncover new features of adhesion site assembly. *Dev Biol* 308, 294–308.
- Dumbauld DW, Lee TT, Singh A, Scrimgeour J, Gersbach CA, Zamir EA, Fu J, Chen CS, Curtis JE, Craig SW, et al. (2013). How vinculin regulates force transmission. *Proc Natl Acad Sci USA* 110, 9788–9793.
- Efron B, Tibshirani R (1993). *An Introduction to the Bootstrap*. Boca Raton, FL: Chapman & Hall/CRC.
- Ellis SJ, Goult BT, Fairchild MJ, Harris NJ, Long J, Lobo P, Czerniecki S, Van Petegem F, Schock F, Peifer M, et al. (2013). Talin autoinhibition is required for morphogenesis. *Curr Biol* 23, 1825–1833.
- Ellis SJ, Lostchuck E, Goult BT, Bouaouina M, Fairchild MJ, Lopez-Ceballos P, Calderwood DA, Tanentzapf G (2014). The Talin head domain reinforces integrin-mediated adhesion by promoting adhesion complex stability and clustering. *PLoS Genet* 10, e1004756.
- Ellis SJ, Pines M, Fairchild MJ, Tanentzapf G (2011). In vivo functional analysis reveals specific roles for the integrin-binding sites of Talin. *J Cell Sci* 124, 1844–1856.
- Ezratty EJ, Bertaux C, Marcantonio EE, Gundersen GG (2009). Clathrin mediates integrin endocytosis for focal adhesion disassembly in migrating cells. *J Cell Biol* 187, 733–747.
- Ezratty EJ, Partridge MA, Gundersen GG (2005). Microtubule-induced focal adhesion disassembly is mediated by dynamin and focal adhesion kinase. *Nat Cell Biol* 7, 581–590.
- Franco-Cea A, Ellis SJ, Fairchild MJ, Yuan L, Cheung TY, Tanentzapf G (2010). Distinct developmental roles for direct and indirect Talin-mediated linkage to actin. *Dev Biol* 345, 64–77.
- Friedland JC, Lee ML, Boettiger D (2009). Mechanically activated integrin switch controls  $\alpha_5\beta_1$  function. *Science* 323, 642–644.
- Gallant ND, Michael KE, Garcia AJ (2005). Cell adhesion strengthening: contributions of adhesive area, integrin binding, and focal adhesion assembly. *Mol Biol Cell* 16, 4329–4340.
- Geiger B, Bershadsky A, Pankov R, Yamada KM (2001). Transmembrane crosstalk between the extracellular matrix–cytoskeleton crosstalk. *Nat Rev Mol Cell Biol* 2, 793–805.
- Geiger B, Spatz JP, Bershadsky AD (2009). Environmental sensing through focal adhesions. *Nat Rev Mol Cell Biol* 10, 21–33.
- Goult BT, Zacharchenko T, Bate N, Tsang R, Hey F, Gingras AR, Elliott PR, Roberts GC, Ballestrem C, Critchley DR, et al. (2013). RIAM and vinculin binding to Talin are mutually exclusive and regulate adhesion assembly and turnover. *J Biol Chem* 288, 8238–8249.
- Grabbe C, Zervas CG, Hunter T, Brown NH, Palmer RH (2004). Focal adhesion kinase is not required for integrin function or viability in *Drosophila*. *Development* 131, 5795–5805.
- Himmel M, Ritter A, Rothemund S, Pauling BV, Rottner K, Gingras AR, Ziegler WH (2009). Control of high affinity interactions in the Talin C terminus: how Talin domains coordinate protein dynamics in cell adhesions. *J Biol Chem* 284, 13832–13842.
- Horwitz A, Duggan K, Buck C, Beckerle MC, Burridge K (1986). Interaction of plasma membrane fibronectin receptor with Talin—a transmembrane linkage. *Nature* 320, 531–533.
- Humphrey JD, Dufresne ER, Schwartz MA (2014). Mechanotransduction and extracellular matrix homeostasis. *Nat Rev Mol Cell Biol* 15, 802–812.
- Ingber DE (2008). Tensegrity and mechanotransduction. *J Bodyw Mov Ther* 12, 198–200.
- Janostiak R, Pataki AC, Brabek J, Rosel D (2014). Mechanosensors in integrin signaling: the emerging role of p130Cas. *Eur J Cell Biol* 93, 445–454.
- Kanchanawong P, Shtengel G, Pasapera AM, Ramko EB, Davidson MW, Hess HF, Waterman CM (2010). Nanoscale architecture of integrin-based cell adhesions. *Nature* 468, 580–584.
- Lavelin I, Wolfenson H, Patla I, Henis YI, Medalia O, Volberg T, Livne A, Kam Z, Geiger B (2013). Differential effect of actomyosin relaxation on the dynamic properties of focal adhesion proteins. *PLoS One* 8, e73549.
- Liu S, Calderwood DA, Ginsberg MH (2000). Integrin cytoplasmic domain-binding proteins. *J Cell Sci* 113, 3563–3571.
- Maartens AP, Brown NH (2015). The many faces of cell adhesion during *Drosophila* muscle development. *Dev Biol* 401, 62–74.
- Macagno JP, Diaz Vera J, Yu Y, MacPherson I, Sandilands E, Palmer R, Norman JC, Frame M, Vidal M (2014). FAK acts as a suppressor of RTK-MAP kinase signalling in *Drosophila melanogaster* epithelia and human cancer cells. *PLoS Genet* 10, e1004262.
- McCann RC, Craig SW (1999). Functional genomic analysis reveals the utility of the I/LWEQ module as a predictor of protein: actin interaction. *Biochem Biophys Res Commun* 266, 135–140.
- Montana ES, Littleton JT (2004). Characterization of a hypercontraction-induced myopathy in *Drosophila* caused by mutations in Mhc. *J Cell Biol* 164, 1045–1054.
- Oakes PW, Beckham Y, Stricker J, Gardel ML (2012). Tension is required but not sufficient for focal adhesion maturation without a stress fiber template. *J Cell Biol* 196, 363–374.
- Oakes PW, Gardel ML (2014). Stressing the limits of focal adhesion mechanosensitivity. *Curr Opin Cell Biol* 30, 68–73.
- Papushveva E, Heisenberg CP (2010). Spatial organization of adhesion: force dependent regulation and function in tissue morphogenesis. *EMBO J* 29, 2753–2768.
- Parsons JT, Horwitz AR, Schwartz MA (2010). Cell adhesion: integrating cytoskeletal dynamics and cellular tension. *Nat Rev Mol Cell Biol* 11, 633–643.
- Pasapera MA, Schneider IC, Rericha E, Schlaepfer DD (2010). Myosin II activity regulates vinculin recruitment to focal adhesions through FAK-mediated paxillin phosphorylation. *J Cell Biol* 188, 877–890.
- Pines M, Das R, Ellis SJ, Morin A, Czerniecki S, Yuan L, Klose M, Coombs D, Tanentzapf G (2012). Mechanical force regulates integrin turnover in *Drosophila* in vivo. *Nat Cell Biol* 14, 935–943.
- Pines M, Fairchild MJ, Tanentzapf G (2011). Distinct regulatory mechanisms control integrin adhesive processes during tissue morphogenesis. *Dev Dyn* 240, 36–51.
- Puklin-Faucher E, Sheetz MP (2009). The mechanical integrin cycle. *J Cell Sci* 122, 179–186.

- Roca-Cusachs P, Iskratsch T, Sheetz MP (2012). Finding the weakest link: exploring integrin-mediated mechanical molecular pathways. *J Cell Sci* 125, 3025–3038.
- Roca-Cusachs P, Sunyer R, Trepast X (2013). Mechanical guidance of cell migration: lessons from chemotaxis. *Curr Opin Cell Biol* 25, 543–549.
- Sawada Y, Tamada M, Dublin-Thaler BJ, Cherniavskaya O, Sakai R, Tanaka S, Sheetz MP (2006). Force sensing by mechanical extension of the Src family kinase substrate p130Cas. *Cell* 127, 1015–1026.
- Schiller HB, Friedel CC, Boulengue C, Fässler R (2011). Quantitative proteomics of the integrin adhesome show a myosin II-dependent recruitment of LIM domain proteins. *EMBO Rep* 12, 259–266.
- Schulman VK, Folker ES, Baylies MK (2013). A method for reversible drug delivery to internal tissues of *Drosophila* embryos. *Fly (Austin)* 7, 193–203.
- Seong J, Tajik A, Sun J, Guan JL, Humphries MJ, Craig SE, Shekaran A, García AJ, Lu S, Lin MZ, et al. (2013). Distinct biophysical mechanisms of focal adhesion kinase mechanoactivation by different extracellular matrix proteins. *Proc Natl Acad Sci USA* 110, 19372–19377.
- Smith SJ, McCann RO (2007). A C-terminal dimerization motif is required for focal adhesion targeting of Talin1 and the interaction of the Talin1 I/LWEQ module with F-actin. *Biochemistry* 46, 10886–10898.
- Stricker J, Aratyn-Schaus Y, Oakes PW, Gardel ML (2011). Spatiotemporal constraints on the force-dependent growth of focal adhesions. *Biophys J* 100, 2883–2893.
- Tadokoro S, Shattil SJ, Eto K, Tai V, Liddington RC, de Pereda JM, Ginsberg MH, Calderwood DA (2003). Talin binding to integrin beta tails: a final common step in integrin activation. *Science* 302, 103–106.
- Tanentzapf G, Brown NH (2006). An interaction between integrin and the Talin FERM domain mediates integrin activation but not linkage to the cytoskeleton. *Nat Cell Biol* 8, 601–606.
- Tanentzapf G, Martin-Bermudo MD, Hicks MS, Brown NH (2006). Multiple factors contribute to integrin-Talin interactions in vivo. *J Cell Sci* 119, 1632–1644.
- Tsai PI, Kao HH, Grabbe C, Lee YT, Ghose A, Lai TT, Peng KP, Van Vactor D, Palmer RH, Chen RH, et al. (2008). Fak56 functions downstream of integrin alphaPS3betanu and suppresses MAPK activation in neuromuscular junction growth. *Neural Dev* 3, 26.
- Tzima E, del Pozo MA, Shattil SJ, Chien S, Schwartz MA (2001). Activation of integrins in endothelial cells by fluid shear stress mediates Rho-dependent cytoskeletal alignment. *EMBO J* 20, 4639–4647.
- Wang N, Naruse K, Stamenovi D, Fredberg JJ, Mijailovich SM, Tolić-Nørrelykke IM, Polte T, Mannix R, Ingber DE (2001). Mechanical behavior in living cells consistent with the tensegrity model. *Proc Natl Acad Sci USA* 98, 7765–7770.
- Wolfenson H, Bershadsky A, Henis YI, Geiger B (2011). Actomyosin-generated tension controls the molecular kinetics of focal adhesions. *J Cell Sci* 124, 1425–1432.
- Yuan L, Fairchild MJ, Perkins AD, Tanentzapf G (2010). Analysis of integrin turnover in fly myotendinous junctions. *J Cell Sci* 123, 939–946.
- Zervas CG, Gregory SL, Brown NH (2001). *Drosophila* integrin-linked kinase is required at sites of integrin adhesion to link the cytoskeleton to the plasma membrane. *J Cell Biol* 152, 1007–1018.